Terahertz spectroscopy of optically thick multilayered semiconductor structures

Stephen E. Ralph and S. Perkowitz

Department of Physics, Emory University, Atlanta, Georgia 30322

N. Katzenellenbogen and D. Grischkowsky

IBM T. J. Watson Research Center, Yorktown Heights, New York 10598

Received March 1, 1994; revised manuscript received August 9, 1994

Using freely propagating terahertz radiation, we have measured the complex dielectric constant of optically thick layered materials from 0.2 THz (6.6 cm^{-1}) to 6 THz (200 cm^{-1}). Transmission measurements of a CdTe–adhesive–Si structure have been successfully fitted to a theoretical model over the measurement range. The accuracy of the theoretical fit shows that the technique of time-domain spectroscopy offers advantages over other spectroscopic methods in the extreme far infrared below 200 cm^{-1}. The signal-to-noise capability of our terahertz-spectroscopy technique permits accurate measurement of power transmission coefficients less than 0.001 (absorption coefficients >5000 cm^{-1}) and index variations larger than $\lambda(dn/d\lambda) > 44$, as demonstrated by the accurate fit of our data through the Reststrahlen region of CdTe.

There has recently been a great deal of research demonstrating the generation and the application of pulsed far-infrared (FIR) radiation. Terahertz (THz) radiation results from the transient electric dipole created when a charge is photogenerated within a strong electric field in a semiconductor. Although many materials radiate in the FIR when they are illuminated with ultrashort laser pulses,[1] a particularly efficient source of the broadband radiation relies on the trap-enhanced fields in semi-insulating GaAs.[2] When illuminated with femtosecond-duration laser pulses these sources produce ultrafast synchronous bursts of THz radiation with a continuous frequency spectrum spanning from ~200 GHz (6.6 cm^{-1}) to in excess of 6 THz (200 cm^{-1}). The temporal characteristics of the FIR pulse simultaneously permit a time resolution of <150 fs. These sources, together with high-speed photoconductors used as THz detectors, form the basis of a new method of FIR spectroscopy called time-domain spectroscopy[3] (TDS). The availability of ultrafast FIR pulses allows both the static and the dynamic properties of materials to be observed by use of TDS.

In addition to its ability to provide fast pulses for time-resolved IR research,[4] the new method of time-domain THz spectroscopy offers advantages[5] over other spectroscopic methods in the extreme FIR below 200 cm^{-1}. In this paper we show that TDS can accurately measure the frequency-dependent complex dielectric constant of individual layers within an optically thick multilayer structure. We fitted our TDS experimental data to a detailed model of the complex dielectric constant and found excellent agreement. We also measured the complex dielectric constant for much thicker, single-layer samples of CdTe. The TDS results for these thicker samples compare well with the results obtained from the multilayer samples and the model and expand the spectral range of accurate data.

Our experimental arrangement is identical to that described earlier[6] and consists of a source chip that is excited by 70-fs visible laser pulses (λ = 623 nm) from a 100-MHz colliding-pulse mode-locked laser. For the source chip of semi-insulating GaAs a charged coplanar transmission line provides the dc bias and functions as a submillimeter-wave point-source antenna. The THz radiation is collimated with a dielectric lens attached directly to the back side of the source chip. The freely propagating THz beam is further collimated with a paraboloidal mirror. The receiver is composed of a nearly identical setup, with the only difference being that the semiconductor receiver antenna is typically made of a small photoconducting gap between two lines of a coplanar transmission line fabricated on ion-implanted Si on sapphire.

The receiver antenna photoconductively samples the focused THz radiation by use of a temporally delayed portion of the laser pulse train. To obtain data, the temporal delay between the source excitation and the receiver sampling pulse is scanned during monitoring of the receiver photocurrent, which is proportional to the electric field of the THz waveform. This delay of the TDS is analogous to the delay of the conventional Fourier transform spectroscopy, although here we delay the visible laser pulse train as opposed to the Fourier transform spectroscopy delay of the broadband FIR beam. A reference spectrum that characterizes the THz beam in the experimental setup is first determined by a numerical Fourier transform of the observed time-domain signal without any sample in the THz-beam path. The sample to be measured is then placed in the THz-beam path, and a second spectrum is determined. Fourier analysis of the reference and the sample THz waveforms yields the absorption and the dispersive properties of the sample.

We measured the complex dielectric function of high-

0740-3224/94/122528-05$06.00

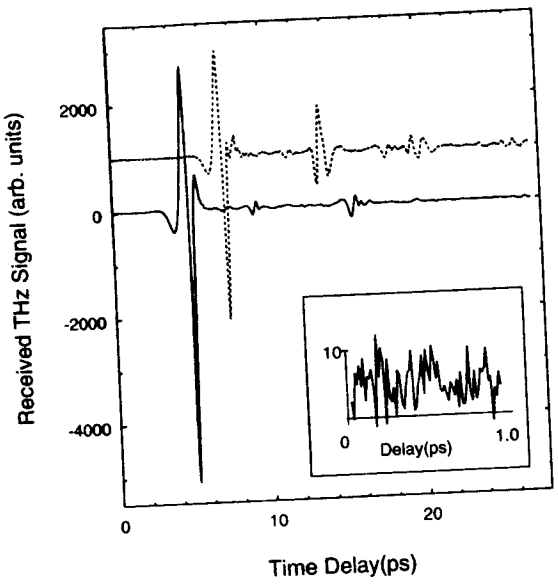

(a)

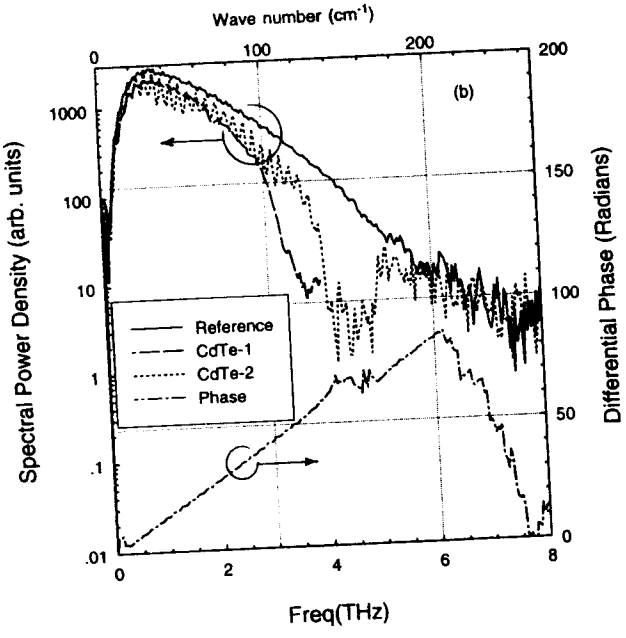

(b)

Fig. 1. (a) Measured THz pulse for both the reference (no sample in beam path, solid curve) and the CdTe multilayer sample (dashed curve). The signal-to-noise capability is exemplified by the expanded portion of the reference signal. (b) Corresponding amplitude and phase spectra of both the reference and the sample time-domain data. CdTe-1, single-layer 320-μm-thick sample; CdTe-2, multilayer structure.

resistivity CdTe by TDS. Although high-resistivity CdTe has a low free-carrier absorption, the reststrahlen region is completely encompassed by our available spectral range. The extremely large absorption ($1/\alpha \approx 1$ μm) near the TO phonon energy of 17 meV (141 cm^{-1}) required that the CdTe samples be mechanically thinned to ~20 μm. The resulting surface was nearly specular. Prior to thinning, the CdTe sample was attached to a 265-μm-thick high-resistivity Si substrate. We then measured the complex transmittance of this multilayer sample, CdTe–adhesive–Si, at normal incidence, using our TDS technique. The adhesive was glycol phthalate (GP). Prior to mounting and thinning the CdTe sample we measured various thicknesses of the same CdTe sample to confirm the measurements of the thin multilayer structure in spectral regions in which the absorption is low. The data show that our technique is capable of resolving the precise CdTe layer thickness and the thin ~12-μm GP adhesive layer.

Figure 1(a) shows the time-resolved data, including both the reference signal and the signal observed with the multilayer sample in the THz-beam path. The inset depicts the system noise by means of the expanded scale. Our mechanical scan of 4 mm corresponds to an optical delay of 27 ps, yielding a frequency resolution of 37 GHz (1.23 cm^{-1}). The sample data clearly exhibit multiple reflections from the sample interfaces; the largest reflection, at a delay of 6 ps with respect to the main signal peak, originates as a result of the Si–air interface. This reflection is to be distinguished from the smaller reflections that originate from the source-chip–Si-lens combination observed equally in the reference signal. The high (>500:1) signal-to-noise ratio of the temporal data is shown by the expanded portion of the reference data. The temporal shift of the sample data with respect to the reference results from the added optical-path length of the sample structure. The TDS technique yields the electric-field amplitude of the received THz signal. Therefore the power spectra, shown in Fig. 1(b) from ~5 to 267 cm^{-1}, are obtained as the magnitude squared of the Fourier transform of the received signal. The corresponding power spectra for the reference, the individual 320-μm-thick CdTe sample (CdTe-1), and the multilayer structure (CdTe-2) are shown. The reduced signal strength evident in both the power spectra and the temporal signal is nearly totally accounted for by Fresnel losses. The interference effects of the multiple reflections are evident in the multilayer sample spectrum. Note that we have plotted power transmission and show a dynamic range larger than 3 orders of magnitude at the peak power near 1 THz. This signal-to-noise capability, achieved with a total scan time of ~20 min, is an advantage of TDS in this spectral range.

In Fig. 1(b) we also show the corresponding cumulative phase data for the multilayer sample data. The phase data are reconstructed from the results of the Fourier analysis, which are inherently modulo 2π. The cumulative phase observed with the sample in the beam path shows the dispersive effects of the CdTe Reststrahlen region centered at 140 cm^{-1}. We mark 200 cm^{-1} as the limit of reliable data because the sample phase data clearly contain an excessive noise component beyond this energy. The small-amplitude oscillations in the phase data further show the effects of interference within the multilayer sample.

The many features of the transmission data arise from both the strong absorption and the multiple reflections from the four interfaces of the sample. The observed transmission therefore depends strongly on the absorption and on the refractive index, both of which are frequency dependent. However, we successfully modeled the transmission of the three-layer structure, using an appropriate dielectric response function $\varepsilon(\omega) = (n + ik)^2$ for the CdTe and the Si. We used the complex refractive

indices, $\varepsilon(\omega) = (n + ik)^2$, to solve numerically the Fresnel equations at the interfaces, including interference effects, to obtain the structure's frequency-dependent transmission coefficient. Briefly, our numerical model is similar to that previously developed[7] and consists of defining a characteristic matrix of the multilayer structure. The wavelength-dependent matrix elements result from the solution to the wave equation. A least-squares-fitting routine was used to vary the IR parameters and the individual layer thicknesses to yield the best fit between calculation and data.

For high-resistivity semiconductors such as those examined here, $\varepsilon(\omega)$ is determined exclusively by lattice vibrations, and, unlike in doped materials,[8,9] the effects of free carriers can be ignored. When modeled as oscillators the effects of phonons yield the familiar Lorentzian line shape given by

$$\varepsilon(\omega) = (n + ik)^2 = \varepsilon(\infty) + \frac{S\omega_{TO}^2}{\omega_{TO}^2 - \omega^2 - i\Gamma\omega},$$

where $\varepsilon(\infty)$ is the high-frequency dielectric constant, S is the oscillator strength, ω_{TO} is the TO photon frequency, and Γ is the damping constant. There are a number of reported sets of values of these parameters for CdTe,[10,11] and most agree closely with the largest variance associated with the damping constant. The TO frequency is 4.23 THz (141 cm^{-1}), and the low transmission between 4 and 5 THz results from strong resonant photon absorption near this frequency. Because Si lacks a TO phonon mode, $\varepsilon(\omega)$ can be simply modeled as a fixed dielectric constant if the contribution of free carriers can be neglected. It has previously been shown that high-resistivity Si ($\rho > 1000\ \Omega$ cm) meets this criterion[12] for our TDS system and is often the material of choice for nonabsorbtive FIR dielectrics. Separately, we measured the FIR transmission of a ~1-mm-thick GP sample and determined that absorption losses were negligible. Therefore the GP adhesive layer was similarly modeled with a constant refractive index and no absorption.

In Fig. 2 the power transmission is plotted together with the results of the model[13] by use of the best-fit parameters listed in Table 1. The three-layer model accurately fits the features of the data, including the closely spaced interference fringes and much of the strong absorption. The peak absorption is apparently too large to measure with this sample thickness. We were unable to fit the data accurately without including the GP interface layer. The fitting was also sensitive to layer thickness variations of $<1.0\ \mu$m. Thus TDS allows us to determine the individual layer thicknesses accurately. An independent measurement with a mechanical thickness gauge yields a total sample thickness of 302 μm compared with the total thickness given by the fitting procedure of 299 μm. Now that the individual layer thicknesses are known, the exact absorption coefficient and refractive index of CdTe can be determined from the TDS data.

Figure 3(a) displays the power absorption coefficient of CdTe obtained from the TDS transmission data by use of the layer thicknesses determined from the fitting procedure. Two sets of data are shown together with the absorption determined from the best-fit model of the complex dielectric constant. One data set, labeled DATA 1a and DATA 1b, represents a composite spectrum that we obtained by joining data from the multilayer structure with data obtained from the single, thick, CdTe sample. The data near the Reststrahlen region corresponds to the multilayer structure, whereas regions of low absorption ($\alpha < 100\ cm^{-1}$) correspond to data obtained from the single CdTe layer. Interference effects are negligible, in one case because of absorption and in the other because of the thicker sample, which produces a reflection outside the range of the temporal scan. The interference-free data of the thick sample exemplifies a particular advantage of TDS: one can eliminate the effects of interference by choosing a suitably narrowed window within the time-domain data. The measured data shown in Fig. 3(a), labeled DATA 2, are obtained by restriction of the analysis window to eliminate the large reflection evident in the multilayer structure data [Fig. 1(a)] at ~16-ps delay. The combination of the large signal-to-noise capability and the temporal-windowing procedure allows the absorption coefficient to be measured over 3 orders of magnitude in a single measurement.

The regions in which multilayer data overlap with the

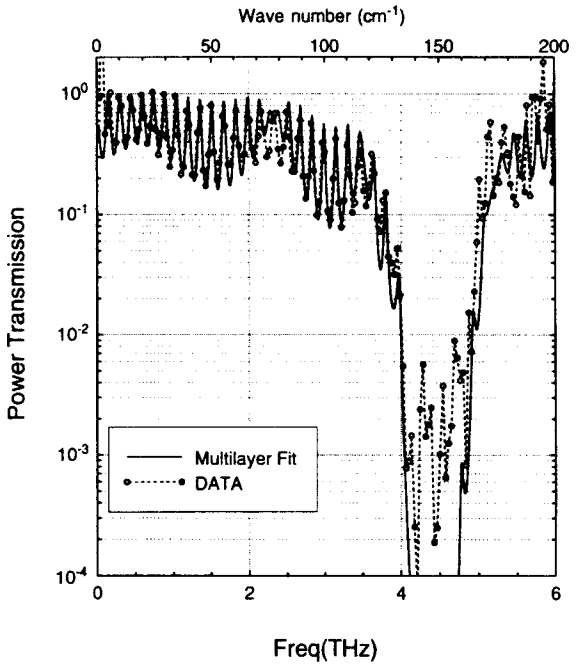

Fig. 2. Measured (circles and dashed curve) power spectra transmission of the multilayer CdTe sample together with the results of the multilayer model (solid curve).

Table 1. Parameters in the Three-Layer CdTe–GP–Si Model Giving the Best Fit to the Measured Transmission Spectrum over 10–180 cm^{-1}[a]

Quantity	CdTe	GP	Si
$\varepsilon(\infty)$	7.15	2.9[a]	11.7
S	2.96	0	0
ω_{TO} (cm^{-1})	140.8	—	—
Γ (cm^{-1})	6.5	—	—
d (μm)	21.0[a]	9.7[a]	265.5[a]

[a]Parameters that were systematically varied.

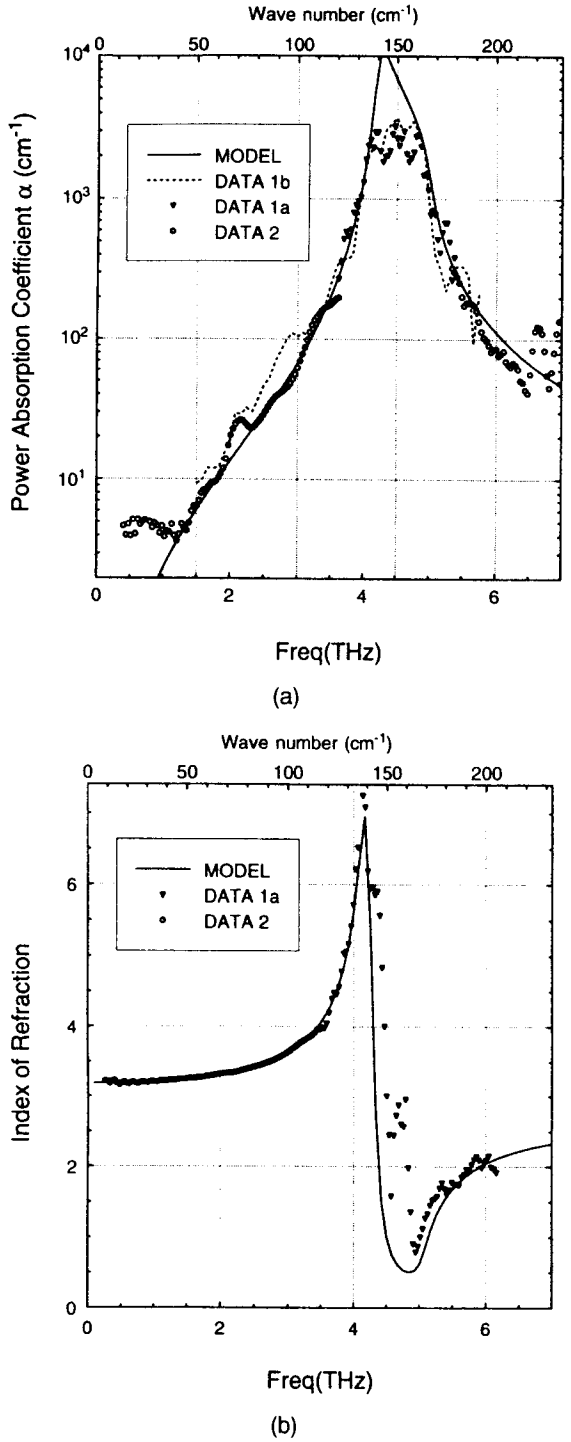

Fig. 3. (a) Power absorption extracted from the measured transmission data by use of the layer thickness and the refractive index determined from the model. (b) Measured refractive index obtained from the transmission data. The solid curves are the theoretical predictions of the model. DATA 1a was obtained from the multilayer sample, and DATA 1b corresponds to the temporally windowed multilayer data. DATA 2 was obtained from the single, thick, CdTe layer.

data obtained from the thicker material show excellent agreement. The agreement with the absorption coefficient determined from the model is also quite good, except that the measured data do not show the largest absorption indicated by the model data at the peak of the phonon absorption. We attribute this discrepancy to the low signal-to-noise capability obtained near the phonon peak. It is likely that the absorption is larger than the measured data suggest. Separately, the pronounced enhancement in absorption near 2.25 THz, as well as the more subtle variations at slightly higher energies, results from multiphonon effects that are not included in our single-harmonic-oscillator model. These multiphonon absorptions and their related index variations result in the slight deviations between the transmission data and the model presented in Fig. 2. In the low-energy region below 1 THz the data should be regarded as an upper bound on the actual absorption coefficient.

In Fig. 3(b) the CdTe refractive index is shown together with the predictions of the model. Because the index is derived from the reconstructed cumulative phase data, in which the absolute phase depends on the phase of each preceding data point, the absolute refractive index depends on the accuracy of every preceding point. The data are in remarkable agreement with the theory, particularly for energies larger than the peak phonon absorption energy. This result suggests that the absorption near the peak of the phonon absorption is not completely obscured by noise and that the phase data remain valid. A close examination of the cumulative phase data reveals that the data near the peak of the absorption are reasonably well defined and are discontinuous at only a few points. This uncertainty in the data near the peak of the phonon absorption leads to the deviation of the measured index from that predicted by the model at frequencies beyond 4.5 THz. The large variation in the index is otherwise easily measured by the TDS technique and is limited only by the frequency resolution of the data because the frequency interval between data points must be much smaller than the range over which the phase changes by $>2\pi$. The large signal-to-noise capability of the TDS technique provides index data that establish the material parameters with high precision. For instance, with the model and the observed data the high-frequency dielectric constant is 7.15 ± 0.05.

It is interesting to consider what effects the CdTe dispersion has on the temporal shape of the THz pulse. Because the spectrally integrated absorption is a small fraction of the total pulse energy, changes in pulse shape may be due to dispersive effects alone. We directly compared the two waveforms and found a sharpening of the initial positive-going portion of the THz waveform. Removing frequency components that are properly phased cannot decrease pulse width; thus the anomalous dispersion of the Reststrahlen region reshapes a portion of the THz pulse to produce a sharper feature by removal of some phase distortion of the experimental setup.

In conclusion, we have demonstrated the use of TDS in the determination of the frequency-dependent complex dielectric constant of CdTe within a multilayer structure. Although the absorption and the index variations go through large extremes in the Reststrahlen region, the TDS technique permits accurate determination of the material parameters within a multilayer structure by suitable modeling of the complex dielectric constant and by proper selection of the temporal window to eliminate unwanted interface reflections. Importantly, the actual absorption and index can be determined.

ACKNOWLEDGMENTS

We thank Lisong Liu for help with the numerical modeling of the data.

REFERENCES AND NOTES

1. X. C. Zhang and D. Auston, Appl. Phys. Lett. **56,** 1011 (1990).
2. S. E. Ralph and D. Grischkowsky, Appl. Phys. Lett. **59,** 1972 (1991).
3. D. Grischkowsky, S. Keiding, M. van Exter, and Ch. Fattinger, J. Opt. Soc. Am. B **7,** 2006 (1990).
4. S. E. Ralph and D. Grischkowsky, in *Materials Research Society Symposium Proceedings*, D. D. Nolte, N. M. Haegel, and K. W. Goossen, eds. (Materials Research Society, Pittsburgh, Pa., 1992), Vol. 261, p. 89.
5. D. Grischkowsky, Opt. Photon. News **3**(5), 21 (1992).
6. For a complete review of the development of TDS and an extensive reference list see Ref. 3.
7. M. Born and E. Wolf, *Principles of Optics*, 6th ed. (Pergamon, Oxford, 1959).
8. N. Katzenellenbogen and D. Grischkowsky, Appl. Phys. Lett. **61,** 840 (1992).
9. S. Perkowitz, *Optical Characterization of Semiconductors: Infrared, Raman, and Photoluminescence Spectroscopy* (Academic, London, 1993), pp. 157–187.
10. S. Perkowitz, J. Electron. Mater. **14,** 551 (1985).
11. E. D. Palik, ed., *Optical Properties of Solids* (Academic, San Diego, Calif., 1985).
12. M. van Exter and D. Grischkowsky, Appl. Phys. Lett. **56,** 1694 (1990), and Ref. 2.
13. S. Perkowitz, Solid State Commun. **84,** 19 (1992).